The Power of Symmetric Spanning Graphs in Public Transport

Irene Heinrich
TU Darmstadt
Darmstadt, Germany
heinrich@mathematik.tu-darmstadt.de

Olli Herrala
Aalto University
Espoo, Finland
olli.herrala1@gmail.com

Piyalee Pattanaik
Aalto University
Espoo, Finland
piyalee.pattanaik@aalto.fi

Philine Schiewe
Aalto University
Espoo, Finland
philine.schiewe@aalto.fi

Abstract

Reducing a given street network to a public transport network is essential for bundling passenger demand and reducing the environmental impact of mobility. Here, both the operators' budget and the passengers' routing costs have to be considered. We introduce a new integer programming model for designing routing-cost-minimal public transport networks in circular cities leveraging their symmetry. In an extensive computational study, we compare generic and symmetric sub-networks structurally, show that the newly introduced model can be solved orders of magnitude faster than generic models and determine that the routing-cost gap between symmetric and generic sub-networks can be disregarded for most budgets.

Keywords

combinatorial optimization, network design, OR applications, price of symmetry, transport network modeling

1 Introduction

Passenger-friendly and cost-efficient public transport supplies are an important step towards climate-friendly mobility [4, 11, 15]. By bundling passenger demand, the distance covered by vehicles can be greatly reduced compared to individual motorized mobility. Therefore, it is necessary to carefully consider which parts of a street network should be used for public transport: On the one hand, using the whole network would result in shorter travel times for passengers (called *routing costs*), high investments (called *building costs*) and achieve little bundling of demand. On the other hand, using a very sparse network results in high routing costs, low building costs, and high bundling of demand.

Spanning subgraphs are sparser substructures of the network that maintain the reachability of the original network. Nevertheless, the routing distances in the sparser network can be greatly increased. Finding a spanning subgraph that is sufficiently sparse while not inducing excessively large distances is an important problem in both theory and practical applications [1–3, 7, 8].

As detailed in [7], using *spanning graphs* to reduce the size of a street network can help achieve a balance between building and routing costs: *Generalized optimum requirement graphs (GORGs)* are spanning graphs that minimize the routing costs for a given building costs budget.

In this work, we consider circular city layouts [14] (called *orb-webs*, see Figure 1) and compare generic GORGs [7] to *symmetric* ones, in particular, subgraphs that are subdivided orb-webs. While generic GORGs allow for larger solution spaces, i.e., for smaller routing costs given a building costs budget, symmetric solutions are more structured, see Figure 1. Thus, they promote fairness (passengers occupying the same structural position in the given network will face the same situation in the sparser network; for example, all suburbs are treated equally) and simplify subsequent planning stages [5], such that integrated solution approaches become feasible [12].

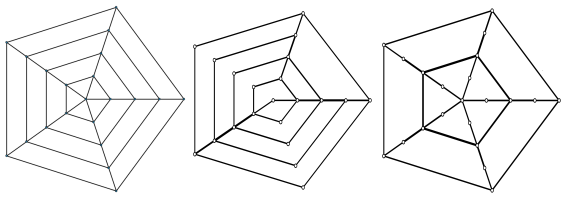

Figure 1: Example for a circular city, i.e., a (5×5)-orb-web (left), with corresponding generic (middle) and symmetric GORG (right).

We exploit the smaller solution space by introducing a new, compact integer programming formulation for finding optimal symmetric GORGs. In an extensive computational study, we analyze the *price of symmetry* [10] and the structure of both symmetric and generic GORGs for two cost functions and various demand scenarios.

2 Preliminaries

For $\ell \in \mathbb{N}$, we set $[\ell] = \{1, 2, \dots, \ell\}$ and $[\ell]_0 = \{0, 1, 2, \dots, \ell\}$.

Graphs. For a graph $G = (V(G), E(G))$ with edge costs $c\colon E(G) \to \mathbb{R}_{\geq 0}$, the length of a shortest u-v path in G with respect to c is the *distance* of u and v and is denoted by $d_G(u, v)$. We set $c_e := c(e)$ for each edge $e \in E(G)$. A subgraph H of G is *spanning* if $V(H) = V(G)$, the edge costs are inherited from G and $d_H(u, v)$ denotes the length of a shortest u-v path in H.

Orb-webs. For $r, s \in \mathbb{N}_{\geq 1}$ the $(r \times s)$-*orb-web* $W_{r,s}$ is a graph consisting of r disjoint rings which are arranged concentrically around the *center* z of a subdivided star of diameter $2r$. More precisely, we define the i-th *ring* of $W_{r,s}$ as $R_i := v_{i,1}v_{i,2} \dots v_{i,s}v_{i,1}$ for each $i \in [r]$ and the j-th *spoke* of $W_{r,s}$ as $S_j := zv_{1,j}v_{2,j} \dots v_{r,j}$ for $j \in [s]$. Then

$$W_{r,s} = \bigcup_{i \in [r]} R_i \cup \bigcup_{j \in [s]} S_j.$$

Observe that this union is not a vertex-disjoint union but every edge of $W_{r,s}$ is contained in exactly one of the subgraphs $R_1, \dots, R_r, S_1, \dots, S_s$. If the edge is contained in a ring (spoke),

INOC '26, Liège (Belgium)

10.48786/inoc.2026.20

then we call it a *ring-edge* (*spoke-edge*). Note that we use $z = v_{0,j}$ for $j \in [s]$.

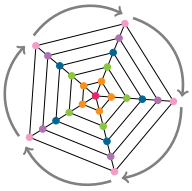

Figure 2: A (5×5)-orb-web. Edges joining vertices of the same (different) colour are ring-edges (spoke-edges). The gray arrows indicate the rotational symmetry.

Cost functions. In this paper we consider a large variety of *symmetric cost functions* which respect the symmetries of orb-webs. Two examples for symmetric cost functions on an $(r \times s)$-orb-web $W_{r,s}$ are:

- *unit costs* where the cost function is set to 1 on each edge of $W_{r,s}$, and
- *Euclidean costs* where we choose a plane embedding of $W_{r,s}$ and take the Euclidean distance of two neighbouring vertices as their cost. The embedding is chosen such that the vertices of a same ring are positioned regularily on a circle with center z.

We restrict the input data to rotationally symmetric instances and, in particular, to symmetric cost functions. Hence, for each $i \in [r]$ there is a constant c_i^r such that $c_e = c_i^r$ for each $e \in E(R_i)$ and a constant c_i^s such that $c_e = c_i^s$ for each edge e connecting the rings R_{i-1} and R_i.

3 The symmetric GORG problem

3.1 Evaluation metrics

Consider an orb-web $W_{r,s}$ with costs c and passenger demand $a_{u,v}$, $u, v \in V(W_{r,s})$. For a spanning subgraph H of $W_{r,s}$, we evaluate

- the *building costs*
$$c(H) = \sum_{e \in E(H)} c_e$$
representing the operators' perspective and
- the *routing costs*
$$r(H) = \sum_{u,v \in V(H)} d_H(u,v) a_{u,v}$$
representing the passengers' perspective.

3.2 Complexity

We define the decision version of the symmetric generalized optimum requirement graph problem as follows.

SYMMETRIC GORG

Input: an orb-web $W_{r,s}$, passenger demand $a_{u,v}$ for $u, v \in V(W_{r,s})$, rotationally symmetric cost function c, a budget K, and a bound B.

Question: Is there a subset $\mathcal{R} \subseteq \{1, \dots, r\}$ such that the building costs of the corresponding symmetric spanning graph $H = \bigcup_{j \in [s]} S_j \cup \bigcup_{i \in \mathcal{R}} R_i$ do not exceed K and the routing costs do not exceed B?

We call the rings R_i, $i \in \mathcal{R}$, *active*.

THEOREM 3.1. SYMMETRIC GORG *is NP-complete.*

PROOF SKETCH. We show that SYMMETRIC GORG is NP-hard via a polynomial time reduction of KNAPSACK to SYMMETRIC GORG.

Given a Knapsack instance with items $(w_i, z_i)_{i=1}^n$, capacity W', and value V', we polynomially construct a symmetric GORG instance on an orb-web with $2n$ rings. The instance is constructed such that odd rings R_{2i-1}, $i \in [n]$, are active in each feasible solution and an active even ring R_{2i}, $i \in [n]$, represents choosing item i. Since KNAPSACK is NP-complete, see [6, 9], this implies that SYMMETRIC GORG is NP-hard.

For the completeness observe that checking whether the building and routing costs do not exceed the respective bounds can be done in time polynomial in the size of the input. □

For the optimization version of this problem, we minimize B while K is constant.

3.3 Leveraging symmetry

We simplify the computation of routing costs $r(H)$ by exploiting H's symmetry: Two origin-destination pairs $(v_{r_1,s_1}, v_{r_2,s_2})$, $(v_{r_3,s_3}, v_{r_4,s_4})$ have the same shortest path length if they start on the same ring $(r_1 = r_3)$, end on the same ring $(r_2 = r_4)$ and origin and destination are separated by the same number of spokes, i.e., $\min\{|s_1 - s_2|, s - |s_1 - s_2|\} = \min\{|s_3 - s_4|, s - |s_3 - s_4|\}$. Observe that we compute the minimum here as the shortest path that can be clockwise or counterclockwise. Thus, we can bundle these OD pairs as

$$\mathrm{OD}_{r_1,r_2,k} = \{(v_{r_1,s_1}, v_{r_2,s_2}) \colon \min\{|s_1 - s_2|, s - |s_1 - s_2|\} = k\}$$

where $r_1, r_2 \in [r]_0$, $k \in [\lfloor \frac{s}{2} \rfloor]_0$ and define the demand of the OD group as

$$a_{r_1,r_2,k} = \sum_{(u,v) \in \mathrm{OD}_{r_1,r_2,k}} a_{uv}.$$

Note that for rotationally symmetric costs, there exists a shortest path between any two vertices that contains ring-edges from at most one ring. Thus, computing the routing costs of H reduces to assigning at most one active ring r_3 to each OD group $\mathrm{OD}_{r_1,r_2,k}$ with corresponding path costs

$$c_{r_1,r_2,k,r_3} = \begin{cases} \sum_{i=1}^{r_2} c_i^s, & r_1 = 0 \\ \sum_{i=1}^{r_1} c_i^s, & r_1 \neq 0, r_2 = 0 \\ \sum_{i=1}^{r_1} c_i^s + \sum_{i=1}^{r_2} c_i^s, & r_1, r_2 \neq 0, r_3 = 0 \\ \sum_{\substack{i \in [r_1+1, r_3] \\ \cup [r_3+1, r_1]}} c_i^s + \sum_{\substack{i \in [r_2+1, r_3] \\ \cup [r_3+1, r_2]}} c_i^s + k \cdot c_{r_3}^r, & r_1, r_2, r_3 \neq 0. \end{cases}$$

3.4 Integer programming formulation

We present an integer programming formulation for finding symmetric GORGs on orb-webs. Here, binary variables x_i, $i \in [r]$, model whether ring i is active and binary variables y_{r_1,r_2,k,r_3}, $r_1, r_2, r_3 \in [r]_0$, $k \in [\lfloor \frac{s}{2} \rfloor]_0$, model the assignment of a path using ring r_3 to the OD pair group $\mathrm{OD}_{r_1,r_2,k}$. Note that $y_{r_1,r_2,k,0}$ represents using a path via the center, i.e., not using any ring-edges.

$$
\begin{aligned}
\min \quad & \sum_{r_1=0}^{r}\sum_{r_2=0}^{r}\sum_{k=0}^{\lfloor \frac{s}{2} \rfloor} a_{r_1,r_2,k} \cdot \sum_{r_3=0}^{r} c_{r_1,r_2,k,r_3} \cdot y_{r_1,r_2,k,r_3} \\
\text{s.t.} \quad & \textstyle\sum_{i=1}^{r} s \cdot c_i^r \cdot x_i \leq K', \\
& \textstyle\sum_{r_3=0}^{r} y_{r_1,r_2,k,r_3} = 1 \qquad r_1, r_2 \in [r]_0, k \in \left[\left\lfloor \tfrac{s}{2} \right\rfloor\right]_0, \\
& y_{r_1,r_2,k,r_3} \leq x_{r_3} \qquad r_1, r_2 \in [r]_0, r_3 \in [r], k \in \left[\left\lfloor \tfrac{s}{2} \right\rfloor\right], \\
& x_i \in \{0,1\} \qquad i \in [r], \\
& y_{r_1,r_2,k,r_3} \in \{0,1\} \qquad r_1, r_2, r_3 \in [r]_0, k \in \left[\left\lfloor \tfrac{s}{2} \right\rfloor\right]_0.
\end{aligned}
$$

Here, the first constraint models the budget accounting for the spoke edges, i.e., $K' = K - \sum_{j=1}^{s} r \cdot c_j^s$, the second constraint models the assignment of paths to the OD groups and the third one restricts the assignment to active rings.

3.5 Price of symmetry

In order to compare symmetric and generic GORGs, we compute the *price of symmetry* following [10]. Let H, H_{sym} be optimal generic and symmetric GORGs for an orb-web G with budget K. Then the price of symmetry is defined as the relative gap

$$\text{PoS} = \frac{r(H_{\text{sym}}) - r(H)}{r(H)}.$$

Note that the price of symmetry is always non-negative, and zero if $r(H) = r(H_{\text{sym}})$. Thus, the lower the price of symmetry is, the better generic GORGs can be approximated by symmetric GORGs.

4 Experimental evaluation

We experimentally evaluate the performance of symmetric GORG compared to generic GORG for asymmetric demands. The implementations are done on the Triton cluster of Aalto University with an Intel(R) Xeon(R) CPU E5-2680 v3 @ 2.50GHz with 4GB memory using Gurobi Optimizer version 12.0.2 within the LinTim software framework [13].

4.1 Data

For the evaluation, we generate orb-webs of different sizes and consider two types of symmetric cost functions. For Euclidean costs, we generate orb-webs $W_{r,s}$ with $r, s \in \{4, 6, 8, 10\}$. For unit costs, we generate orb-webs $W_{r,s}$ with $r \in \{1, 2, 3, 4, 5\}$ and $s \in \{3, 4, 5\}$. For each orb-web $W_{r,s}$, we consider budget values $K_0, K_1, \ldots, K_r$, ranging from the cost of all spoke edges (K_0) to the cost of all edges in $W_{r,s}$ (K_r). Furthermore, we construct a sequence of $r+1$ asymmetric demand scenarios $A^z = A^{R_0}, A^{R_1}, \ldots, A^{R_r}$ to capture variations in passenger demand in the network, see Figure 3. In each scenario A^{R_i}, all vertices except one vertex in ring R_i are assigned a uniform baseline demand, while the remaining vertex has a higher demand. The demand $a_{u,v}^{R_i}$ is then computed via a gravity model implemented in LinTim [13], using the network distance in the orb-web, i.e., $d_{W_{r,s}}(u, v)$. In total, we thus solve 1374 instances of the symmetric and generic GORG problem, respectively.

4.2 Runtime

First, we compare the runtime of the newly introduced IP formulation for symmetric GORGs with the one-to-many formulation for generic GORGs presented in [7]. Table 1 summarizes the solver time of the IPs as well as the percentages of instances solved to optimality within the one-hour time limit. It is evident

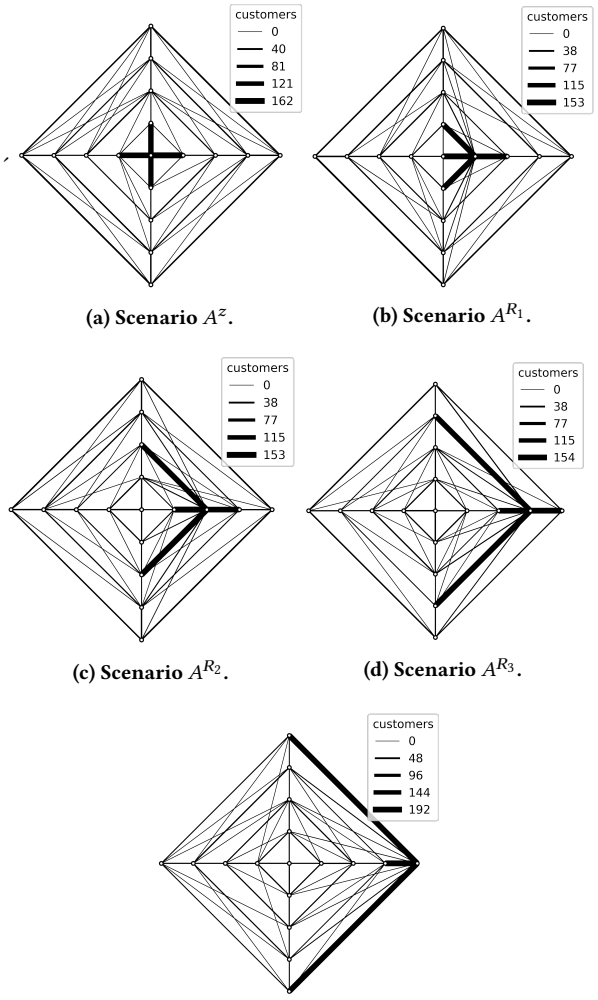

(a) Scenario A^z. **(b) Scenario A^{R_1}.**

(c) Scenario A^{R_2}. **(d) Scenario A^{R_3}.**

(e) Scenario A^{R_4}.

Figure 3: Demand scenarios for a (4×4)-orb-web. The line width of an edge uv corresponds to the demand $a_{u,v}^{R_i}$.

that the symmetric GORG model can be solved orders of magnitude faster than the generic one. For symmetric GORG, the maximum runtime over all instances with Euclidean costs is under two seconds and for unit costs under 0.05 seconds. Note that for Euclidean costs, instances are up to (10×10)-orb-webs, while unit costs are only considered for up to (5×5)-orb-webs. In contrast, 2.1% and 1.3% of generic GORG instances cannot be solved to optimality in the one-hour time limit for Euclidean and unit costs, respectively. Note further that the mean runtime increases to 279 and 119 seconds, compared to less than 0.1 seconds for the symmtric GORG. When considering the price of symmetry in Section 4.3, we exclude instances with positive optimality gap.

Table 1: Runtime for generic and symmetric GORG. % opt. refers to the percentage of instances solved to optimality within the one-hour time limit

	Euclidean costs			unit costs		
	mean	max	% opt.	mean	max	% opt.
gen.	279.09	3600.36	97.9	118.56	3600.18	98.7
sym.	0.07	1.97	100.0	0.01	0.05	100.0

Figure 4 details the influence of the network structure under the two cost models. Here, the vertical axis represents the number of spokes s, while the horizontal axis indicates the number of rings r. Darker shading corresponds to higher solver runtime. We observed that for generic GORGs, the runtime increases markedly with both the number of spokes and rings. For Euclidean costs, increasing the number of spokes has a higher effect than increasing the number of rings while both have a similar effect for unit costs. As expected, the number of spokes barely influences the runtime for symmetric models, where decisions are solely based on activated rings.

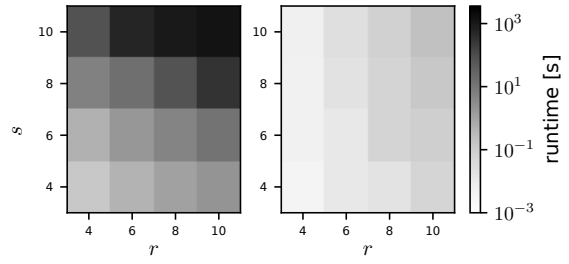

(a) Euclidean costs: generic (left) vs symmetric (right).

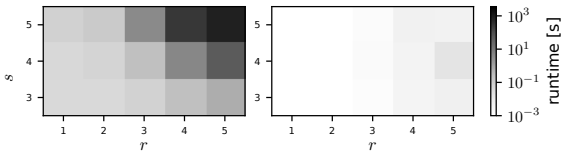

(b) Unit costs: generic (left) vs symmetric (right).

Figure 4: Runtime heatmaps in seconds.

4.3 Price of symmetry

Although symmetry constraints substantially reduce computational effort, it is crucial to assess whether this restriction leads to a significant loss in solution quality.

Table 2 shows that for Euclidean costs, the symmetric GORG is optimal for the generic GORG problem in more than half of the considered instances. Furthermore, the mean price of symmetry is under 0.01 and the maximum 0.16. While symmetric demand concentrated in the center (A^z) can be approximated especially well (74% of instances have PoS=0), asymmetric demand concentrated towards the outskirts (A^{R_r}) is hardest to approximated by symmetric solutions (28% of instances have PoS=0). The highest price of symmetry is attained with the lowest budget K_0 at 0.16, with a maximum PoS of 0.05 for all other budgets.

For unit costs, generic GORGs cannot be approximated as well by symmetric ones. Here, 47% of the instances have PoS=0, the mean price of symmetry increases to 0.05 and the maximum to 2.27. However, this is mostly due to the lowest considered budget (K_0) where only 39% of the instances have PoS=0. When considering all other budgets, 49% of instances have PoS=0, the mean price of symmetry falls to 0.01 and the maximum price of symmetry falls to 0.4. This shows that for reasonable budgets, symmetric solutions can approximate generic solutions very well.

Figures 5 and 6 illustrate the price of symmetry as a function of demand and the configuration of the network. The y-axis reports the price of symmetry (PoS), while the x-axis specifies the demand scenarios ($A^z, \ldots, A^{R_r}$). Within each demand scenario, the sequence of plotted points corresponds to progressively relaxed budget constraints $K_0, \ldots, K_r$.

Table 2: Price of symmetry. % opt. refers to the percentage of instances with PoS=0.

	Euclidean costs			unit costs		
	mean	max	% opt.	mean	max	% opt.
all	0.006	0.159	50.4	0.047	2.274	47.2
A^z	0.001	0.013	74.0	0.022	0.656	69.0
A^{R_1}	0.008	0.159	61.5	0.070	0.841	47.7
A^{R_r}	0.008	0.100	28.1	0.102	2.274	30.4
K_0	0.025	0.159	57.3	0.272	2.274	38.9
$K > K_0$	0.004	0.051	49.5	0.011	0.415	48.5

For Euclidean costs, see Figure 5, we observe that the price of symmetry decreases with an increasing number of rings in the network but increases with increasing number of spokes. The special status of symmetric demand scenarios (A^z) with PoS<0.01 is evident as well as a high influence of the minimum budget (K_0). However, all other demand scenarios ($A^{R_1}, \ldots, A^{R_r}$) show similar price of symmetry values.

For unit costs, see Figure 6, we observe a different pattern. Here, the price of symmetry increases with increasing number of rings, and with demand scenarios emphasizing outer rings. It decreases slightly wih increasing number of spokes. At the lowest budget levels (K_0), the price of symmetry attains its highest values and decreases monotonously with the sharpest decline from K_0 to K_1.

The different behaviour of the price of symmetry for Euclidean and unit costs is due to the costs of adding rings. In the Euclidean setting with fixed spoke-edge costs, ring-edges become increasingly expensive. Thus, outer ring edges are less likely to be part of a shortest path, unless the number of spokes increases and subdivides the outer rings into cheaper edges.

4.4 Structure of optimal solutions

For analyzing the structure of optimal solutions, we transform an orb-web into a compressed linear representation (see Figure 7). Here, the ring-(spoke-)edges are condensed into vertices (edges) along a vertical axis, where the lowest vertex represents the center z. We denote generic (symmetric) solutions using blue (red) vertices and solid blue (dotted red) edges. The shades of vertices (edges) indicate the activation of the corresponding ring-(spoke-)edges in the original graph. The deepest shade denotes the activation of all corresponding ring-(spoke-)edges. Conversely, a lighter colour (or no colour) signifies the activation of some (or none) of the edges. Note that in a symmetric solution, all spoke-edges are active.

Figure 8 illustrates the symmetric and generic GORGs of (4×4)-orb-webs across different demand scenarios. For each scenario, the left-most (right-most) pair of linear representations corresponds to the lowest (highest) budget K_0 (K_4). We furthermore illustrate the price of symmetry for the solution below.

Under Euclidean costs, see Figure 8 (left), the solutions for symmetric and generic GORGs coincide in almost all cases. Deviations occur only when the demand is concentrated in outer rings, i.e., for A^{R_3} and A^{R_4}. In these solutions, all spoke-edges are consistently included, and rings are activated progressively in a concentric manner, starting from the innermost ring and expanding outward as the budget increases. This pattern reflects

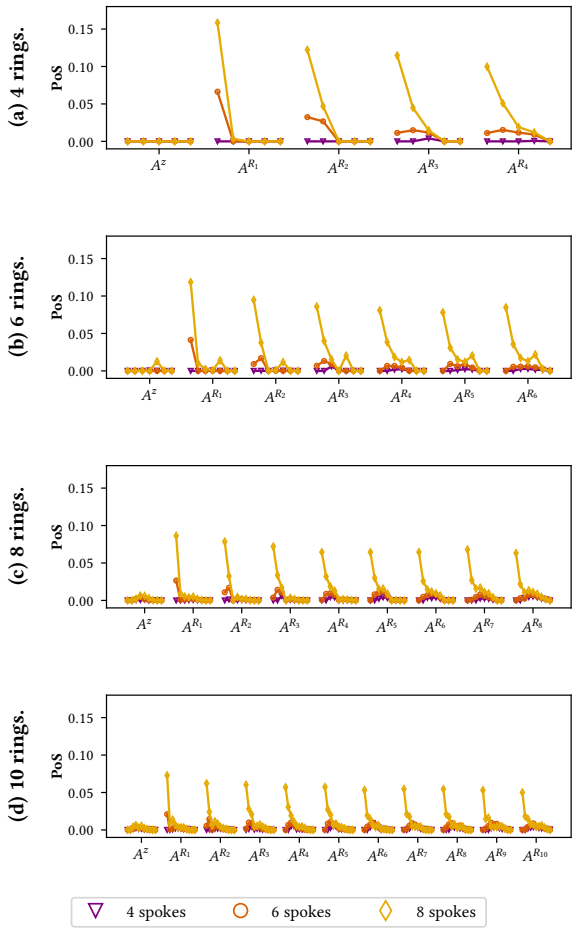

Figure 5: Price of symmetry for Euclidean costs. For each demand scenario, the left-most (right-most) points represent the lowest (highest) budget.

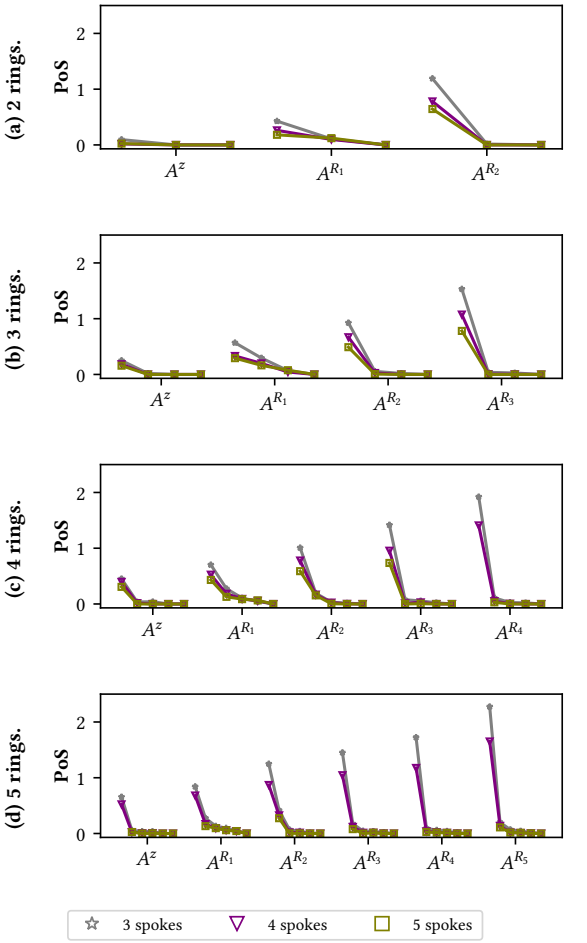

Figure 6: Price of symmetry for unit costs. For each demand scenario, the left-most (right-most) points represent the lowest (highest) budget.

the cost structure, where outer rings are more expensive due to longer distances, and highlights a hierarchical strategy for network expansion: inner-ring connections are prioritized to efficiently satisfy demand before allocating resources to outer rings. Note that even for demand scenarios A^{R_3} and A^{R_4}, the price of symmetry is at most 0.001, indicating that the quality of the generic and symmetric solutions are almost identical.

Under unit costs, see Figure 8 (right), the picture changes significantly. Symmetric and generic GORGs diverge, highlighting the effect of design flexibility when edge costs are uniform. These differences are particularly profound at lower budget levels, i.e., for K_0 where the price of symmetry ranges from 0.5 to 1.5. As expected, the highest divergence between symmetric and generic solutions can be observed for the most asymmetric demand scenario A^{R_4}, where the lowest bugdet K_0 leads to building a maximal number of ring-edges in the generic GORG.

Note that for moderate budgets $K \in \{K_1, K_2, K_3\}$ the structure of generic and symmetric solutions is notably different while the price of symmetry is low. This shows a considerable opportunity for using symmetric solutions in practice: With minimal losses in routing costs, we can switch to a symmetric solution that is easier to memorize and can be perceived as more fair, thus contributing to higher adoption of public transport.

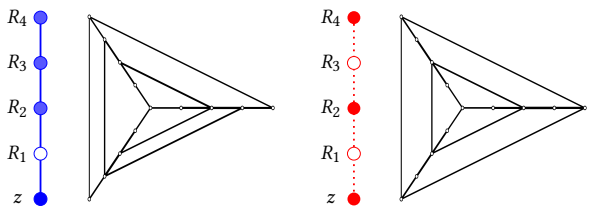

Figure 7: Linear representation for (4×3)-orb-webs. Left: generic GORG, right: symmetric GORG.

5 Conclusion and future work

In this paper we studied the impact of symmetry constraints in the generalized optimum requirement graph problem (GORG) within the context of public transport network design. We established the computational complexity of the Symmetric GORG problem, proving NP-completeness, and quantified the efficiency loss induced by symmetry through the price of symmetry. Our theoretical and experimental results show that, while symmetry may restrict feasible design choices, its cost is often negligible in practice, particularly under Euclidean cost structures. Non-zero price of symmetry values arise primarily in low-budget settings. Through these findings we provide a motivation for the use of

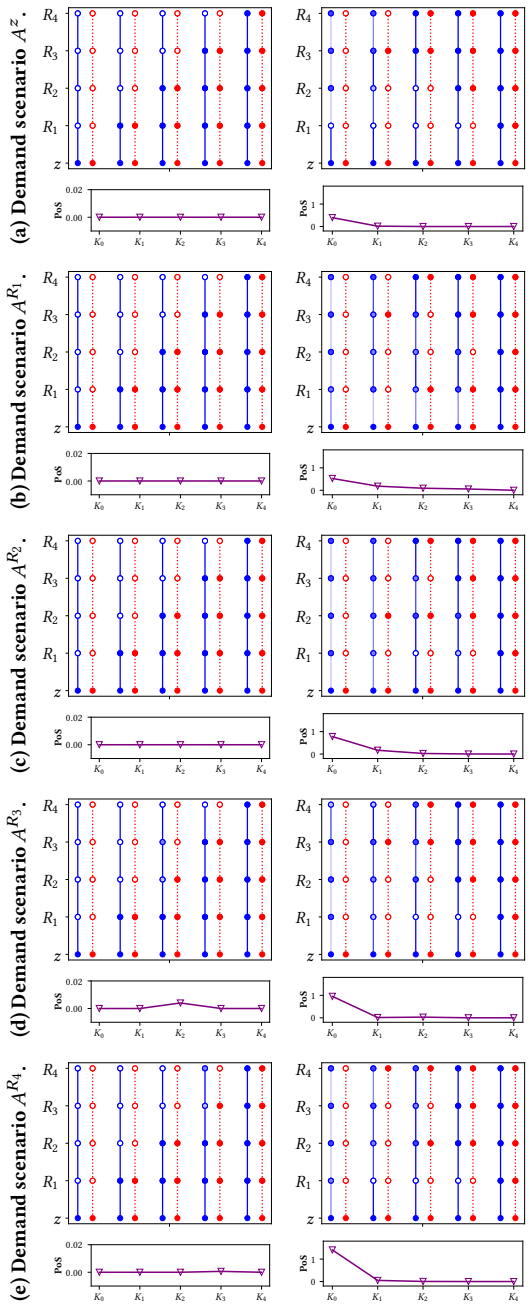

Figure 8: Comparison of (4×4)-orb-web solutions: Euclidean costs (left) and unit costs (right).

symmetric models in real-world transport systems and also highlight conditions under which symmetry can be imposed without significant performance loss. This motivates the investigation of symmetric models in additional settings, such as grid-like networks, to promote fair, sustainable and efficient public transport network design.

Acknowledgments

This work was supported by the Research Council of Finland (Flagship of Advanced Mathematics for Sensing Imaging and Modelling 359181).

References

[1] Júlia Baligács, Yann Disser, Irene Heinrich, and Pascal Schweitzer. 2026. Exploration of graphs with excluded minors. *J. Comput. Syst. Sci.* 156 (2026), 103725. doi:10.1016/J.JCSS.2025.103725

[2] Fritz Bökler, Markus Chimani, and Henning Jasper. 2025. Simple Approximations for General Spanner Problems. In *Approximation and Online Algorithms - 23rd International Workshop, WAOA 2025, Warsaw, Poland, September 18-19, 2025, Proceedings (Lecture Notes in Computer Science, Vol. 16077)*, Jannik Matuschke and José Verschae (Eds.). Springer, 48–63. doi:10.1007/978-3-032-06706-7_4

[3] Fritz Bökler and Henning Jasper. 2024. Complexity of the multiobjective minimum weight minimum stretch spanner problem. *Math. Methods Oper. Res.* 100, 1 (2024), 65–83. doi:10.1007/S00186-024-00850-7

[4] Umweltbundesamt Deutschland, Axel Stein, Dennis Günthel, René Naumann, Simon Hänel, Stephan Ulle, Heike Gading, Jantje Struß, and Dennis Steinke. 2025. Abschlussbericht: Luftreinhaltung und Klimaschutz durch Stärkung des ÖPNV.

[5] Markus Friedrich, Alexander Migl, Alexander Schiewe, Magdalena Schilling, and Anita Schöbel. 2022. Improving the Solvability of Public Transport Problems Using System Routes. In *15th International Conference on Advanced Systems in Public Transport, CASPT 2022, Tel Aviv, Israel, November 6-10, 2022.*

[6] M. R. Garey and David S. Johnson. 1979. *Computers and Intractability: A Guide to the Theory of NP-Completeness.* W. H. Freeman.

[7] Irene Heinrich, Olli Herrala, Philine Schiewe, and Topias Terho. 2023. Using Light Spanning Graphs for Passenger Assignment in Public Transport. In *23rd Symposium on Algorithmic Approaches for Transportation Modelling, Optimization, and Systems, ATMOS 2023, Amsterdam, The Netherlands, September 7-8, 2023 (OASIcs, Vol. 115)*, Daniele Frigioni and Philine Schiewe (Eds.). Schloss Dagstuhl - Leibniz-Zentrum für Informatik, 2:1–2:16. doi:10.4230/OASICS.ATMOS.2023.2

[8] T. C. Hu. 1974. Optimum Communication Spanning Trees. *SIAM J. Comput.* 3, 3 (1974), 188–195. doi:10.1137/0203015

[9] Richard M. Karp. 1972. Reducibility Among Combinatorial Problems. In *Proceedings of a symposium on the Complexity of Computer Computations, held March 20-22, 1972, at the IBM Thomas J. Watson Research Center, Yorktown Heights, New York, USA (The IBM Research Symposia Series)*, Raymond E. Miller and James W. Thatcher (Eds.). Plenum Press, New York, 85–103. doi:10.1007/978-1-4684-2001-2_9

[10] Berenike Masing, Niels Lindner, and Ralf Borndörfer. 2022. The Price of Symmetric Line Plans in the Parametric City. *Transportation Research Part B: Methodological* 166 (2022), 419–443. doi:10.1016/j.trb.2022.03.004

[11] Audronė Minelgaitė, Renata Dagiliūtė, and Genovaitė Liobikienė. 2020. The Usage of Public Transport and Impact of Satisfaction in the European Union. *Sustainability* 12, 21 (2020). doi:10.3390/su12219154

[12] Philine Schiewe and Anita Schöbel. 2022. Integrated optimization of sequential processes: General analysis and application to public transport. *EURO J. Transp. Logist.* 11 (2022), 100073. doi:10.1016/J.EJTL.2022.100073

[13] Philine Schiewe, Anita Schöbel, Olli Herrala, Michael Rihlmann, Sarah Roth, Sebastian Albert, Christine Biedinger, Thorsten Dahlheimer, Lena Dittrich, Klara Hoffmann, Sven Jäger, Piyalee Pattanaik, Alexander Schiewe, Moritz Stinzendörfer, and Reena Urban. 2025. Documentation for LinTim 2025.11. 225 pages. https://nbn-resolving.de/urn:nbn:de:hbz:386-kluedo-93118

[14] Patrick Stokkink, André de Palma, and Nikolas Geroliminis. 2023. Carpooling with Transfers and Travel Time Uncertainty. In *11th Symposium of the European Association for Research in Transportation (hEART 2023).*

[15] United Nations. 2015. Transforming Our World: The 2030 Agenda for Sustainable Development. https://sdgs.un.org/sites/default/files/publications/21252030%20Agenda%20for%20Sustainable%20Development%20web.pdf Resolution A/RES/70/1.